TÜBİTAK

Research Article

Full bridge converter based independent phase control of a permanent magnet reluctance generator for wind power conversion systems

Erkan SUNAN[1] , **Fuat KÜÇÜK**[2,*]
[1]Energy Institute, TÜBİTAK Marmara Research Center, Kocaeli, Turkey
[2]Department of Electrical Engineering, İstanbul Technical University, İstanbul, Turkey

Abstract: A Permanent Magnet Reluctance Generator (PMRG) possesses important features such as simplicity and low cost. Absence of rotor winding allows the generator to run in a wide speed range. The PMRG may have potential to be used in wind power conversion systems. An asymmetric half bridge (AHB) converter may be acceptable as a classical converter topology for PMRGs and offers independent phase control. The AHB converter with a torque ripple minimization-assisted maximum power point tracking algorithm not only provides significant torque ripple reduction on the mechanical side but also allows conversion of maximum wind energy to electrical energy. The major drawback is that the AHB converter is not commercially available as a single module; hence, manual construction by combining discrete components is required. Instead, this work introduces for the first time, the use of a full bridge (FB) converter for independent phase control of the PMRG. The main advantage is that the FB converter is commercially available as a standard intelligent power module. In order to obtain unidirectional current as in the AHB converter, modified delta configuration of the phase windings has been used. The experimental results under fixed and variable wind speed conditions confirm the effectiveness of the proposed control-converter configuration.

Key words: Permanent magnet reluctance generator, full bridge converter, independent phase control, torque ripple minimization, wind power, maximum power point tracking

1. Introduction

The roles of renewable energy systems (RESs) in worldwide electric power generation have been increasing incredibly because of the fact that they use free and clean resources and cause almost zero emission. Wind Power Conversion Systems (WPCSs) are the fastest developing and most promising ones among the RESs [1], and thus currently have the largest utilization [2]. Although wind power technology has been reliable for a long time, the cost of power generation is still not competitive with that of any fossil based energy conversion systems. New attempts to develop new type generators as well as power electronic circuit topologies are necessary for reducing manufacturing costs and increasing maintainability. A Switched Reluctance Generator (SRG) comes to the fore with its simplicity and low cost. Absence of rotor windings increases the capability of producing electrical energy in a wide speed range. The SRG is characterized by low-speed high-torque operation, and therefore it can meet the expectations of WPCSs [3,4]. A permanent magnet reluctance generator (PMRG) can be regarded as a special type SRG with magnets on the stator yoke. Unlike SRGs, it does not require any excitation circuit or external power source. Various types of PMRGs have been designed for small-scale

---

*Correspondence: fkucuk@itu.edu.tr

applications [5–7]. These are often controlled by a combination of a diode bridge and a buck-boost converter [8–10]. The common drawback of this configuration is that large torque ripples due to the nature of the PMRG cannot be suppressed. This is because the converter configuration has only one control parameter, that is, duty ratio. Torque ripples cause acoustic noise, vibrations, and stresses on the mechanical side of the wind turbine and may cause serious failure or damage in the WPCS [11,12]. However, an asymmetric half bridge (AHB) converter, which is accepted to be the traditional converter topology for switched reluctance (SR) machines, provides independent phase control of each phase and hence multiple degree of flexibility, which makes it suitable for applying a torque control strategy. Recently, it has been demonstrated an AHB converter accompanied with a maximum power point tracking (MPPT) algorithm can be used to control an SRG [13,15]. Moreover, combination of MPPT with a torque control strategy for an AHB converter driven PMRG has been introduced [16] and has been experimentally verified [17]. This may be regarded as an important milestone in developing a PMRG driven WPCS.

Although the AHB converter provides many benefits, its three phase form as a single module is not commercially available. The user must manually construct the converter by manually combining discrete components such as six semiconductor switches and their gate drivers and protection circuits. Therefore, the constructed converter especially suffers from low reliability and high cost.

Including the same amount of switches, a full bridge (FB) converter is commercially available as intelligent power modules (IPMs) and has wide use in the field of AC machine drives. The IPM is an all-in-one compact package including the switches, gate drives, and protection circuit. It offers lower size and cost as well as fewer connections (only three wires for three phase) to the machine. Valuable works demonstrate that FB converters can also be used to control SR machine [18,21]. Clothier et al. introduced independent phase control of a switched reluctance motor (SRM) by using the FB converter and diodes placed in series with the phase winding [22]. Later, the performance of the same converter configuration was analyzed for different types of SRM [23]. Although valuable works to achieve independent phase control by using an FB converter have been reported, to the best of our knowledge neither of them has been focused on integrating the converter with a torque ripple control strategy and MPPT. There is one attempt to combine an FB converter with torque ripple control and MPPT [24], which does not provide independent phase control.

Our paper presents, for the first time, independent phase control of the PMRG by FB converter. The converter and modified delta configuration does not only have the benefits of using standard IPM and cheap diodes but also provides an opportunity to apply MPPT and torque ripple minimization (TRM). The control strategy with the FB based converter configuration has been experimentally applied to the PMRG driven WPCS under constant and variable wind speed conditions.

2. Basics of a PMRG based WPCS

A PMRG based WPCS can be examined in two parts: the PMRG and the wind turbine system. Each part is explained in the following.

2.1. The PMRG

The PMRG employed in this research is illustrated in Figure 1. The generator has 6/4 poles and thus rotational symmetry is $90°$. Two magnets are located diametrically on the stator yoke. The PMRG is eventually a nonlinear electromagnetic system and can be described with the following equations:
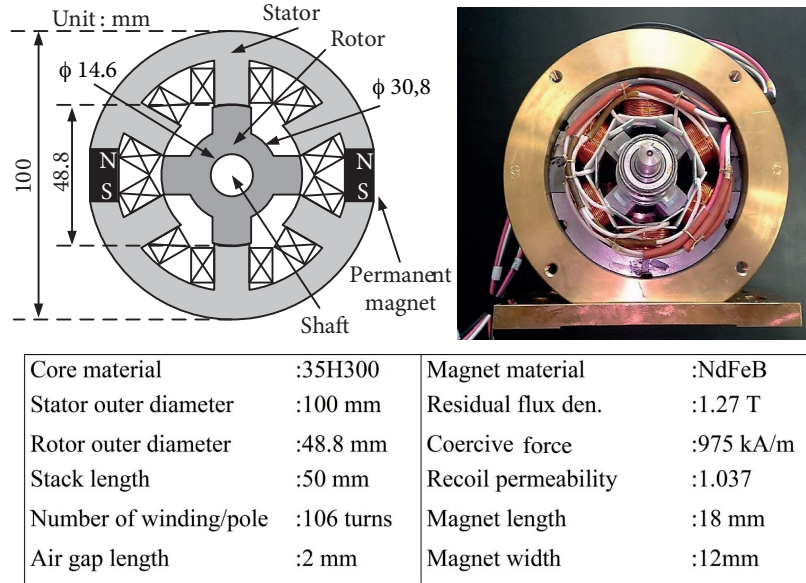
Figure 1. Technical specifications of the PMRG used in this research.

$$\psi_{\mathrm{k}} = \int (v_k - R_k i_k) dt \tag{1}$$

$$\tau_k = \left. \frac{\partial W_k'}{\partial \theta} \right|_{i_k = const}, \tag{2}$$

where v_k, R_k, i_k, and ψ_k are the voltage, resistance, current, and flux linkage of the kth phase, respectively, and θ is the rotor position. W_k' and τ_k are, respectively, the coenergy and phase torque.

ψ_k represents the nonlinearity of the magnetic circuit. Assuming no magnetic saturation, phase torque developed in a classical SRG is purely current reluctance torque and may be expressed as

$$\tau_k = \frac{1}{2} i_k^2 \frac{dL_k}{d\theta}, \tag{3}$$

where L_k is the inductance of the kth coil. In the case of PMRG, torque has permanent magnet reluctance torque as well as mutual torque components besides current reluctance torque:

$$\tau_k = \frac{1}{2} i_k^2 \frac{dL_k}{d\theta} - \frac{1}{2} \varphi_m^2 \frac{dR_{gk}}{d\theta} + N i_k \frac{d\varphi_m}{d\theta}, \tag{4}$$

where R_{gk} is the air gap reluctance and φ_m is the flux due to the permanent magnet. It is obvious that the sum of each phase torque results in the total torque developed in the machine:

$$\tau = \sum_{k=A,B,C} \tau_k \tag{5}$$

Eq. (4) may make the calculation easier. However, the variation in air gap reluctance with respect to the rotor position is still necessary. Since the variation is not readily available, a PMRG model for finite element analysis (FEA) should be constructed [5]. The results can be used for further calculation of air gap reluctance [17].

2.2. Wind turbine system

The power that can be extracted from the wind is strongly depending on the wind and wind turbine characteristics. The relationship can be expressed as

$$P_m = \frac{1}{2}\rho\, C_p(\lambda, \beta) R^2 V_w^3, \tag{6}$$

where C_p is the power coefficient of the turbine. R and V_w respectively represent the blade radius and the wind speed.

The tip speed ratio (TSR) is defined as the ratio between the linear speed of the tip of the blade and the wind speed. The linear speed can be written in terms of the angular speed, and thus the TSR can be expressed as

$$\lambda = \frac{\omega_m R}{V_w} \tag{7}$$

The torque generated in the wind turbine is

$$T_m = \frac{1}{2}\rho\, C_t(\lambda, \beta) R^3 V_w^2, \tag{8}$$

where C_t is torque coefficient. The relationship between C_t and C_p is given as

$$C_t(\lambda, \beta) = \frac{C_p(\lambda, \beta)}{\lambda} \tag{9}$$

The characteristic of a wind turbine is often given with the curves of mechanical power vs. angular speed $(P_m - \omega_m)$ at fixed wind speeds. Figure 2 displays such a characteristic for the wind turbine utilized in this work.
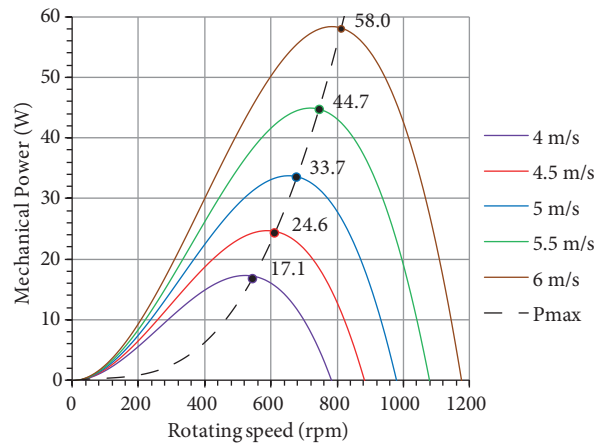

Figure 2. Mechanical power curves of the wind turbine system.

3. TRM-assisted MPPT control of an AHB converter

3.1. TRM-assisted MPPT control

RESs often utilize some MPPT control techniques to capture maximum power from the source. One of the best-known MPPT techniques is called the hill climb search (HCS) [25]. In this method, the algorithm searches

for the maximum power point (MPP) of the corresponding power curve of the wind turbine. This technique provides independency from the wind turbine characteristic while searching for the MPP [26]. The overall diagram of torque ripple minimization (TRM)-assisted MPPT control is given in Figure 3. The control concept can be explained by dividing it into two parts: the MPPT algorithm and the TRM.
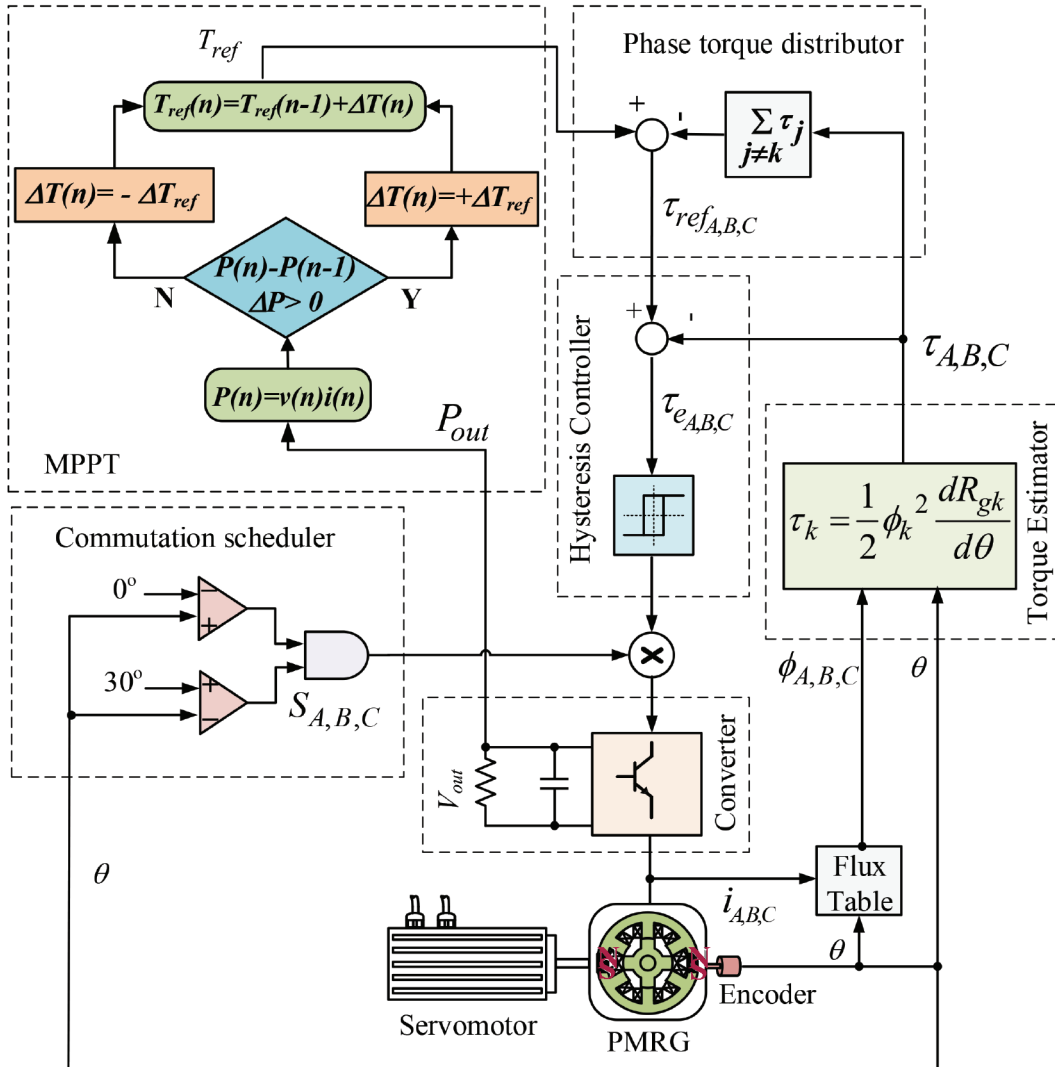

Figure 3. Complete diagram of torque ripple minimization-assisted MPPT control.

3.1.1. The MPPT algorithm

The power measured from the load side is taken as an input by the MPPT algorithm. It observes power change, ΔP, in each step. Current variation in the reference torque is defined by the power change between the two consecutive measurements. If the power variation is positive, the sign of the reference torque variation, ΔT_{ref}, remains the same. Otherwise, the sign is negated. The updated value and sign of ΔT_{ref} is used for determining the reference torque T_{ref}. The MPPT output is indicated as reference torque because it is used as an input to the torque control algorithm rather than generating gate signals directly. The procedure of defining MPPT

output can be expressed as

$$\Delta T_{ref}(n) = \Delta T_{ref}(n-1) \cdot sign(\Delta P) \tag{10}$$

$$T_{ref}(n) = T_{ref}(n-1) + \Delta T_{ref}(n), \tag{11}$$

where n refers to the step of MPP searching. Note that ΔT_{ref} and T_{ref} require initialization at the beginning of MPP searching. The magnitude of ΔT_{ref} is always constant, that is, only the sign changes according to the power change.

3.1.2. The TRM

The MPPT is accompanied by a TRM algorithm to suppress possible effects of torque ripples. In order to provide reference torque for each phase from the MPPT output, a torque distributor is used. As seen in Figure 3, the distributor finds the reference phase torque by taking the difference between the sum of estimated torques of other phases and total reference torque. For example, τ_{refB} is obtained by subtracting the sum of τ_A and τ_B from T_{ref}. Each estimated phase torque is then subtracted from the corresponding reference phase torque to find phase torque error, τ_e. The hysteresis controller receives each phase torque error and generates required signals to suppress torque ripples in a predetermined band. A commutation scheduler defines which portion of the generated signals will be used. The required gate signals are simply generated from multiplying the output of the hysteresis controller with the output of the commutation scheduler.

3.2. AHB converter and switching

The AHB converter topology is suitable for applying TRM-assisted MPPT control to the PMRG based WPCS (Figure 4). Thus, energy conversion is achieved at its maximum point without stressing the components of the mechanical side. Such a system has been simulated and experimentally tested, respectively, in [21] and [22]. The switching scheme of the semiconductor switches in a three phase AHB converter is displayed in Figure 5 to be able to make a comparison with that of the proposed switching scheme.

4. Proposed control strategy converter configuration

The combination of TRM assisted-MPPT algorithm and AHB converter has proved its effectiveness in independent phase control of PMRGs. What is expected from a converter topology is that it should be easily found as a single package. The AHB converter may be considered to be the classical converter topology for the SRG family; however, it is not commercially available. Therefore, manual construction including a drive circuit is required. Instead, a 3-phase FB converter may be reasonable because its IPM package has widespread use with AC machines. In order to achieve independent phase control of the PMRG by FB converter, the winding configuration needs to be modified.

4.1. Modified delta-FB converter configuration and switching

Unlike the AHB converter, the current flow in the FB converter is bidirectional. Thus, independent phase control as in the AHB converter cannot be implemented. However, a modification in the winding configuration may help in successful independent phase control with the FB converter. Such a configuration that allows unidirectional current as in the AHB converter is illustrated in Figure 6. As seen in the figure, a diode is
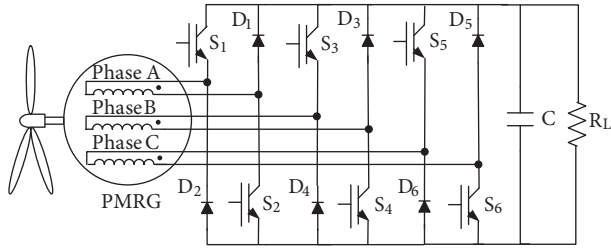
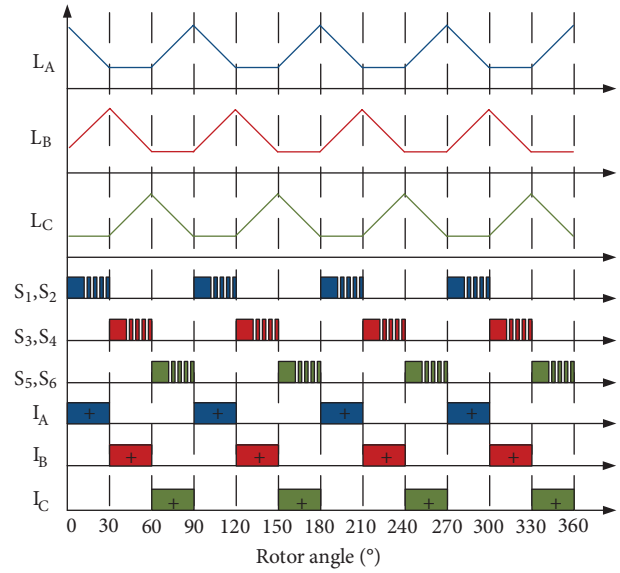**Figure 4**. AHB converter topology for the PMRG based WPCS.

Figure 5. Switching scheme of the AHB converter.
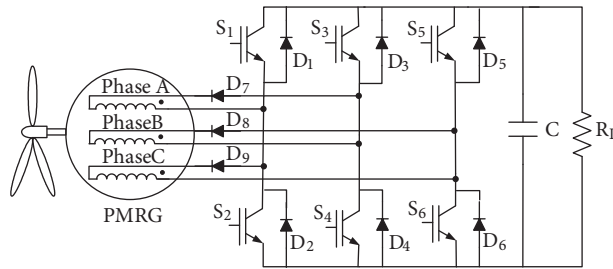

Figure 6. Modified delta-FB converter and configuration for the PMRG.

connected in series with each winding before connecting them in delta form. A star connection cannot be used because it does not allow a closed path for unidirectional current.

The switching scheme of the FB converter is given in Figure 7. The operation of the new scheme can be summarized as follows: when the rotor angle is between $0°$ and $30°$ (first interval), the diodes D_1 and D_4 at the FB side as well as the diode D_7 at the modified delta side are naturally ON because of positive induced voltage in phase A. Thus, the PMRG runs in generating mode (GM). The other diodes D_8 and D_9 at the modified delta side make the current flow only through phase A. During power generation, if suppression of torque ripples is required, the switches S_2 and S_3 are made ON, which forces D_1 and D_4 to become OFF. The D_7 is still ON and the PMRG runs in breaking mode (BM) for a short time. Running BM mode is repeated whenever torque ripple is out of the predefined limits and lasts until the rotor position is out of the first interval. When the rotor angle is between $30°$ and $60°$ (second interval), positive voltage is induced in phase B. Thus, the diodes D_3, D_6, and D_8 are ON for GM whereas S_4, S_5, and D_8 are ON for BM. When the rotor angle is between $60°$ and $90°$ (third interval) then positive voltage is induced in phase C and makes the diodes D_2, D_5, and D_9 naturally ON for GM whereas S_1, S_6, and S_9 are made ON for BM if necessary. After the third interval the electrical period is completed. ON–OFF conditions of all switches and diodes are given for both the AHB converter and modified delta-FB converter in the Table.
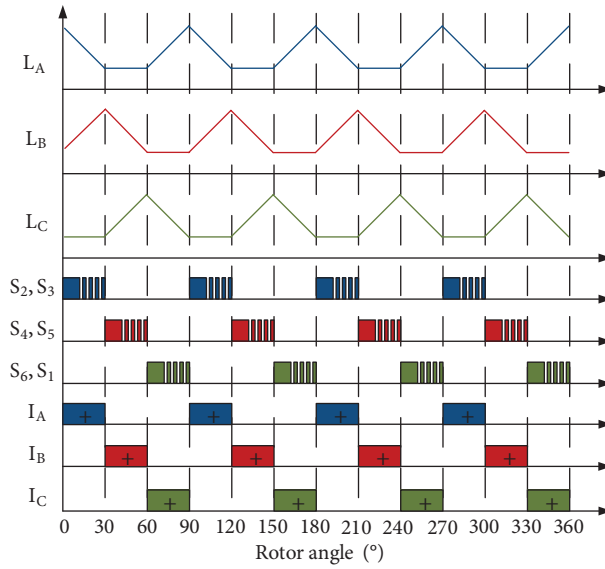
Figure 7. Switching scheme for the 3-phase FB converter.

Table. Overall switching table for both converters.

AHB converter	Rotor mechanical angle (°)						Modified delta+FB converter
	0–30		30–60		60–90		
	GM	BM	GM	BM	GM	BM	
D_1, D_2	ON	OFF	OFF	OFF	OFF	OFF	D_1, D_4, D_7
S_1, S_2	OFF	ON	OFF	OFF	OFF	OFF	S_2, S_3, D_7
D_3, D_4	OFF	OFF	ON	OFF	OFF	OFF	D_3, D_6, D_8
S_3, S_4	OFF	OFF	OFF	ON	OFF	OFF	S_4, S_5, D_8
D_5, D_6	OFF	OFF	OFF	OFF	ON	OFF	D_5, D_2, D_9
S_5, S_6	OFF	OFF	OFF	OFF	OFF	ON	S_1, S_6, S_9

5. Experimental results and discussion

The performance of the new converter configuration and TRM-assisted MPPT control was tested on the PMRG based WPCS. The results are evaluated and compared with those of the AHB converter case. The overall experimental setup is illustrated in Figure 8. In order to explain how the experiment is executed, it seems that a basic diagram for the experimental setup will be useful. Such a diagram is displayed in Figure 9. The TRM-assisted MPPT algorithm was first prepared in MATLAB/Simulink tool. The prepared Simulink file was embedded in a digital processor named dSPACE DS1103 via real time interface (RTI). A computer program named ControlDesk was used to control parameters such as turn-on–turn-off angles of the switches and monitoring the parameters such as rotor position, phase currents, and phase voltages. A computer-controlled servomotor was employed to imitate the dynamic behavior of the wind turbine and rotate the PMRG at the desired speed. A capacitor of 4.7 mF and a resistive load of 50 Ω were selected for the electrical side. Turn-on and turn-off angles of each transistor are respectively set to 0° and 30°. The conditions given above were applied for both converters during the experiments. The performance investigation was carried out under constant speed and variable speed conditions.
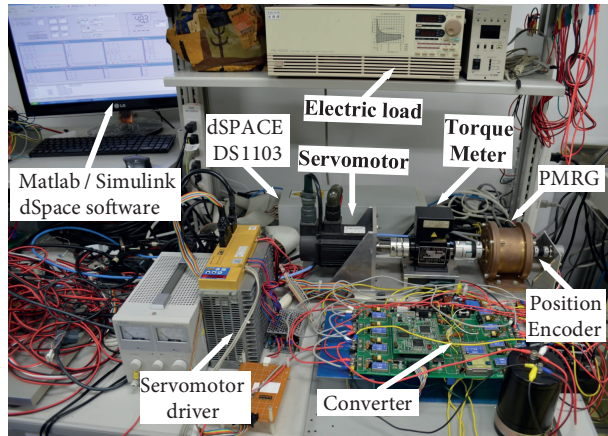
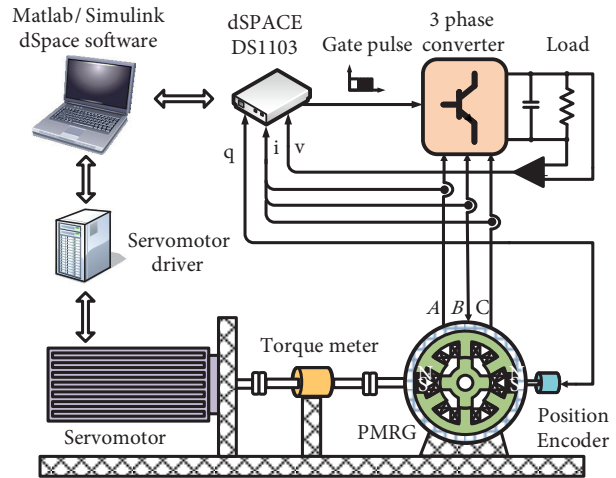**Figure 8**. The overall experimental setup.

Figure 9. Simplified experimental setup.

5.1. Steady state performance

For steady state performance analysis, the wind turbine was exposed to a constant wind speed of 5 m/s. Figure 10 displays the steady state results of AHB converter use. The electrical power output is around 21 W (Figure 10a) and the output power of the wind turbine is about 33.5 W (Figure 10b). According to the power curves given in Figure 2, the WPCS works at its MPP. Torque developed in the machine is settled around 0.47 Nm and varies between 0.58 and 0.22 Nm (Figure 10c), while the PMRG is running at around 675 rpm (Figure 10d). Figure 11 displays the steady state results of modified delta-FB converter use. The electrical power output is around 21 W (Figure 11a) and the output power of the wind turbine is about 33.5 W (Figure 11b). Therefore,
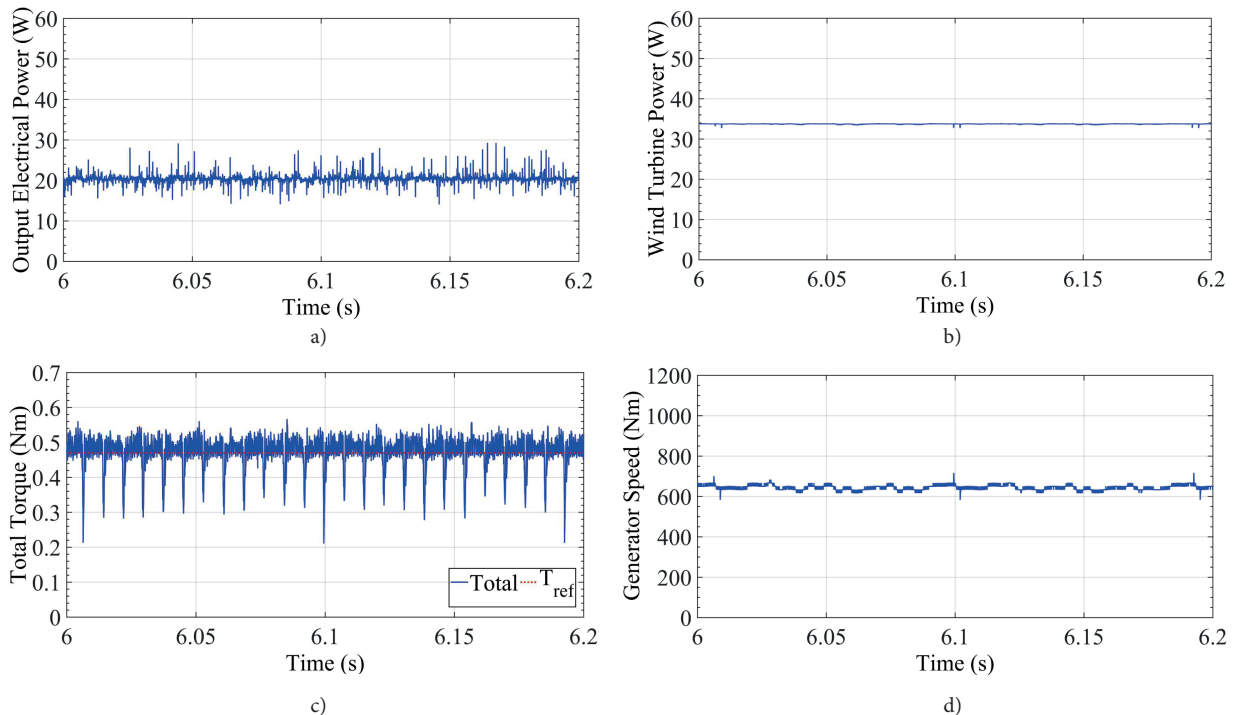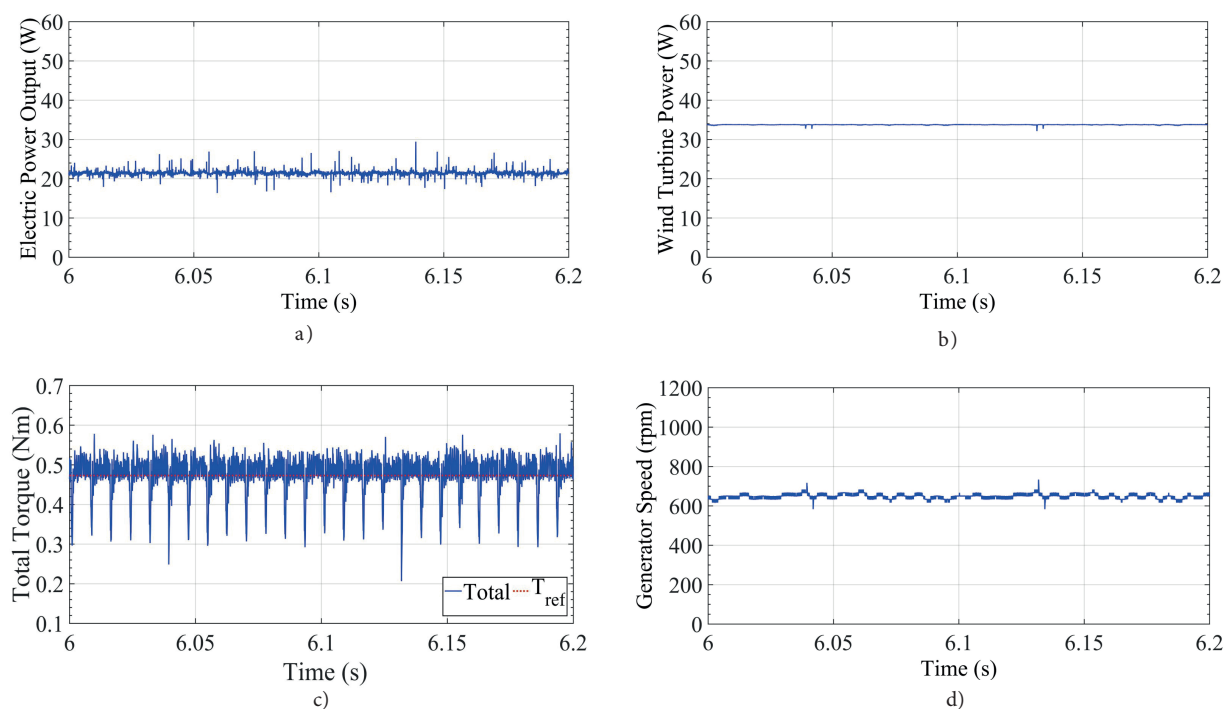

Figure 10. Experimental results of AHB converter use under constant wind speed.

Figure 11. Experimental results of modified delta-FB converter use under constant wind speed.

the WPCS works at its MPP, as in the AHB converter use. Torque is settled at around 0.48 Nm and varies between 0.58 and 0.21 Nm (Figure 11c), while PMRG is running at around 625 rpm (Figure 11d). The system efficiency is 62.7% for both converters.

5.2. Dynamic performance

For dynamic performance analysis, the wind turbine was exposed to a variable wind speed profile. As seen in Figure 12a, the PMRG based WPCS was initially run with the wind speed of 5m/s, then it was reduced to 4.5 m/s, and then increased to 5.5 m/s with a constant step of 0.5 m/s. It is obvious from Figure 12b that the system is always running at around the corresponding MPP of the power curve. Changing the wind speed from 4.5 m/s to 5.5 m/s allows increasing turbine power from 24 W to 43 W, increasing electric power from 14 W to 28 W (Figure 12c). During the wind speed variation, the rotational speed changes from 550 rpm to 800 rpm (Figure 12d).

6. Conclusion

This research introduced, for the first time, the use of a modified delta-FB converter configuration for independent phase control of PMRGs. When the modified delta-FB converter is accompanied by a TRM-assisted MPPT algorithm, significant reduction in torque ripples was obtained while converting wind power to electric energy at its MPP.

The new converter configuration employs a ready-to-use IPM; hence, the AHB converter can be easily replaced by an FB converter. The functionality of the AHB converter is obtained by using modified delta together with the FB converter. The experimental results under steady state and dynamic conditions demonstrate that
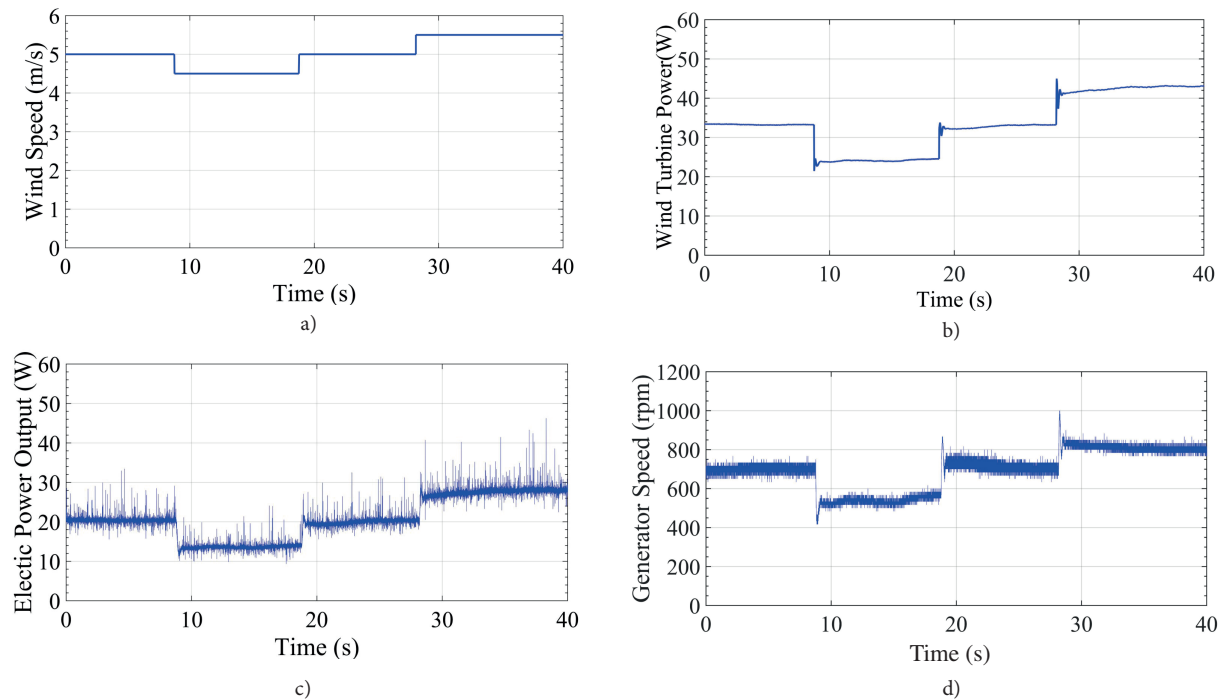
Figure 12. Experimental results of modified delta-FB converter use under variable wind speed.

the proposed control-converter configuration works as effectively as the AHB converter does. It was also shown that independent phase control can also be achieved by a new configuration. Although the PMRG employed in this work has small power, it can still be utilized to show the effectiveness of the proposed control-converter configuration for small-scale applications.

One of the possible drawbacks of the proposed control-converter configuration is that the switching interval of transistors used in the FB converter must be limited to $30°$ to avoid short-circuiting the phases. This problem does not occur in the AHB converter and the switching interval can be extended over $30°$. The other drawback is that the MPPT strategy used in this research may not always be fast enough to catch the MPP of the corresponding power curve in time. This problem is supposed to be solved by using a variable reference torque step rather than using a constant value. Thus, a faster and more efficient MPPT algorithm may be obtained.

References

[1] Ahn JW, Oh SG, Moon JW, Hwang YM. A three-phase switched reluctance motor with two-phase excitation. IEEE T Ind Appl 1999; 35: 1067-1075.

[2] Clothier AC, Mecrow BC. The use of three phase bridge inverters with switched reluctance drives. In: Eighth International Conference on Electrical Machines and Drives; 1–3 September 1997; Cambridge, UK. Stevenage, UK: IET. pp. 351-355.

[3] Datta R, Ranganathan VT. A method of tracking the peak power points for a variable speed wind energy conversion system. IEEE T Energy Conver 2003; 18: 163-168.

[4] Edrington CS, Krishnamurthy M, Fahimi B. Bipolar switched reluctance machines: a novel solution for automotive applications. IEEE T Veh Technol 2005; 54: 795-808.

[5] Goto H, Guo HJ, Ichinokura O. A micro wind power generation system using permanent magnet reluctance generator. In: 13th European Conference on Power Electronics and Applications; 8–10 September 2009; Barcelona, Spain. New York, NY, USA: IEEE. pp. 1-8.

[6] Hasanien HM, Muyeen SM. Speed control of grid-connected switched reluctance generator driven by variable speed wind turbine using adaptive neural network controller. Electr Pow Syst Res 2012; 84: 206-213.

[7] Ichinokura O, Ono T, Takahashi A, Nakamura K, Watanabe T. Three-phase reluctance generator with permanent magnets buried in stator core. In: 12th International Power Electronics and Motion Control Conference; 30 August–1 September 2006; Portoroz, Slovenia. New York, NY, USA: IEEE. pp. 1032-1036.

[8] Kioskeridis I, Mademlis C. Optimal efficiency control of switched reluctance generators. IEEE T Power Electr 2006; 21: 1062-1072.

[9] Koutroulis E, Kalaitzakis K. Design of a maximum power tracking system for wind-energy-conversion applications. IEEE T Ind Electron 2006; 53: 486-494.

[10] Munteanu I, Bratcu AI, Ceanga NA, Cutululis E. Optimal Control of Wind Energy Systems. London, UK: Springer, 2008.

[11] Nakamura K, Ichinokura O. Super-multipolar permanent magnet reluctance generator designed for small-scale wind-turbine generation. IEEE T Magn 2012; 48: 3311-3314.

[12] Nakamura K, Yoshida J, Ichinokura O. Stator-permanent-magnet reluctance generator using ferrite magnet for small-scale renewable energy generation. EPE J 2010; 20: 31-36.

[13] Nasirian V, Kaboli S, Davoudi A. Output power maximization and optimal symmetric freewheeling excitation for switched reluctance generators. IEEE T Ind Appl 2013; 49: 1031-1042.

[14] Peng J, Deng Z, Chen X, Liu Z, Wang X, Wu Y, Cai J. Dynamic analysis of switched reluctance motor in two different control strategies based on three-phase bridge converter. In: International Conference on Applied Superconductivity and Electromagnetic Devices; 25–27 September 2009; Chengdu, China. New York, NY, USA: IEEE. pp. 255-258.

[15] Potgieter JHJ, Kamper MJ. Torque and voltage quality in design optimization of low-cost non-overlap single layer winding permanent magnet wind generator. IEEE T Ind Electron 2012; 59: 2147-2156.

[16] Raza KSM, Goto H, Guo HJ, Ichinokura O. A novel algorithm for fast and efficient maximum power point tracking of wind energy conversion systems. In: 18th International Conference on Electrical Machines; 6–9 September 2008; Vilamoura, Portugal. New York, NY, USA: IEEE. pp. 1-6.

[17] Raza KSM, Goto H, Guo HJ, Ichinokura O. A novel algorithm for fast and efficient speed-sensorless maximum power point tracking in wind energy conversion systems. IEEE T Ind Electron 2011; 58: 29-36.

[18] Somsiri P, Tungpimonrut K, Aree P. Three-phase full-bridge converters applied to switched reluctance motor drives with a modified switching strategy. In: International Conference on Electrical Machines and Systems; 8–11 October 2007; Seoul, South Korea. New York, NY, USA: IEEE. pp. 1563-1568.

[19] Srinivas KN, Arumugam R. Static and dynamic vibration analyses of switched reluctance motors including bearings, housing, rotor dynamics, and applied loads. IEEE T Magn 2004; 40: 1911-1919.

[20] Sunan E, Raza KSM, Goto H, Guo HJ, Ichinokura O. Instantaneous torque ripple control and maximum power extraction in a permanent magnet reluctance generator driven wind energy conversion system. In: The XIX International Conference on Electrical Machines; 6–8 September 2010; Rome, Italy. New York, NY, USA: IEEE. pp. 1-6.

[21] Sunan E, Kucuk F, Raza KS, Goto H, Guo HJ, Ichinokura O. Torque ripple minimization and maximum power point tracking of a permanent magnet reluctance generator for wind energy conversion system. J Renew Sustain Ener 2013; 5: 1-14.

[22] Sunan E, Kucuk F, Goto H, Guo HJ, Ichinokura O. Three-phase full bridge converter controlled permanent magnet reluctance generator for small-scale wind energy conversion systems. IEEE T Energy Conver 2014; 29: 585-593.

[23] Torrey DA. Switched reluctance generators and their control. IEEE T Ind Electron 2002; 49: 3-14.

[24] Vandana R, Nikam S, Fernandes BG. High torque polyphase segmented switched reluctance motor with novel excitation strategy. IET Electr Power App 2012; 6: 375-384.

[25] Xia Y, Ahmed KH, Williams BW. Wind turbine power coefficient analysis of a new maximum power point tracking technique. IEEE T Ind Electron 2013; 60: 1122-1132.

[26] Xiong L, Xu B, Gao H, Xu L. A novel algorithm of switched reluctance generator for maximum power point tracking in wind turbine application. In: International Conference on Sustainable Power Generation and Supply; 6–7 April 2009; Nanjing, China. New York, NY, USA: IEEE. pp. 1-5.